Transition Modeling based on the Dual N-Factor Method for the CRM-NLF Wind Tunnel Configuration

P. Paredes[1] B. Venkatachari[1] M. Choudhari[2] F. Li[2]

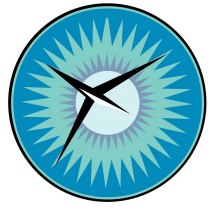
[1]National Institute of Aerospace

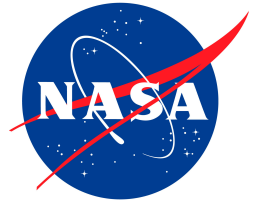
[2]Computational AeroSciences Branch, NASA Langley Research Center

AIAA Aviation 2023

APA-17, Boundary-Layer Transition for Aerodynamic Applications I

9:30AM-11:30AM PDT, Torrey Hills B, San Diego, CA. June 13, 2023

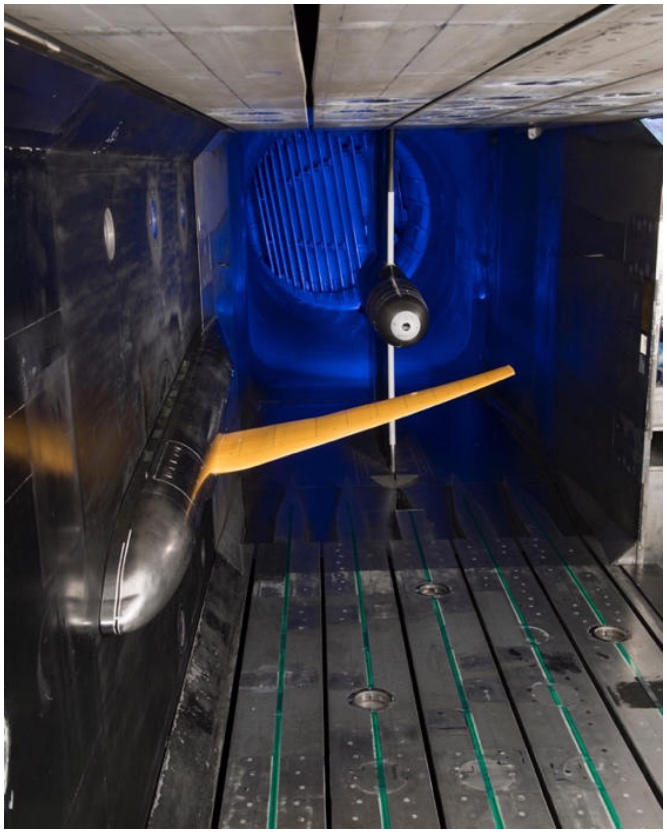




Outline

1. Motivation
2. Theory
3. Results
4. Summary and Concluding Remarks

Common Research Model - Natural Laminar Flow[1]



- CRM is an open geometry representation of a generic transport vehicle
- CRM-NLF includes wing designed for extended natural laminar flow by controlling
  - attachment line contamination and instability
  - crossflow (CF) instability
  - Tollmien-Schlichting (TS) instability
- `https://commonresearchmodel.larc.nasa.gov/crm-nlf`

[1] Richard L. Campbell and Michelle Lynde. *Expanding the natural laminar flow boundary for supersonic transports*. AIAA Paper 2016-4327. 2016. DOI: 10.2514/6.2016-4327.

Objectives

- Systematic methodology for transition prediction and modeling for three-dimensional, transonic wings
- Previous work[2,3,4,5] involving parallel stability computations (LST) for the CRM-NLF has shown that the measured onset of transition can be correlated with TS and CF linear amplification
- Iteratively coupled computational fluid dynamics (CFD) and stability calculations with a dual N-factor criterion:
  - basic state computed by using full Navier-Stokes equations with OVERFLOW 2.3b
  - stability analysis performed by using nonorthogonal PSE with LASTRAC.3d
- Evaluate the predictive performance of the dual *N*-factor criterion[6]
- Provide guidance to improve the physical basis of existing transition models

[2] M. Lynde, R. Campbell, and S. Viken. *Additional findings from the common research model natural laminar flow wind tunnel test*. AIAA Paper 2019-3292. 2019. DOI: 10.2514/6.2019-3292.

[3] J.-S. Fischer, B. Soemarwoto, and E. van der Weide. "Automatic Transition Prediction in a Navier-Stokes Solver Using Linear Stability Theory". In: *AIAA Journal* 59.7 (2021), pp. 2409–2426. DOI: 10.2514/1.J059910.

[4] A. Krumbein, D. Francois, and N. Krimmelbein. "Transport-Based Transition Prediction for the Common Research Model Natural Laminar Flow Configuration". In: *Journal of Aircraft* (2022). DOI: 10.2514/1.C036918.

[5] N. Krimmelbein and A. Krumbein. *Transition prediction for the NASA CRM-NLF with the e^N-method using incompressible and compressible linear stability analysis*. AIAA Paper 2022-1953. 2022. DOI: 10.2514/6.2022-1953.

[6] D. Arnal. "Boundary layer transition: Prediction based on linear theory". In: *Special course on Progress in Transition Modeling. AGARD. R-793.* 1994, pp. 1–62.

Outline

1 Motivation

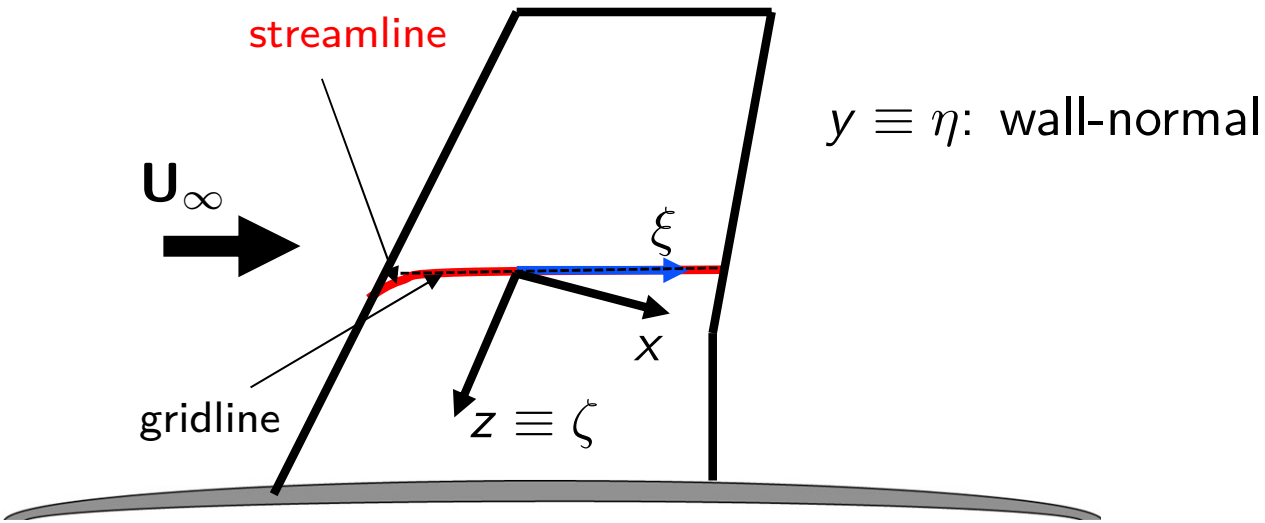
2 Theory

3 Results

4 Summary and Concluding Remarks

Nonorthogonal Parabolized Stability Equations (PSE)

- The NASA LASTRAC.3d solver[7]
- Nonorthogonal PSE along streamlines:
  - definition of coordinates:
    - ξ: streamwise along streamline
    - η: wall normal
    - ζ: spanwise parallel to leading edge
  - allows clear distinction between stationary CF ($\omega = 0$) and planar TS ($\beta = 0$)
  - includes surface curvature and nonparallel mean flow effects



[7] C.-L. Chang. *LASTRAC.3d: Transition Prediction in 3D Boundary Layers*. AIAA Paper 2004-2542. 2004.

The Dual N-factor Criterion[10]

- The logarithmic amplification ratio or N-factor is defined as

$$N(\xi, \omega, \beta) = -\int_{\xi_I}^{\xi} \sigma(\xi', \omega, \beta)\, \mathrm{d}\xi'$$

- Transition onset predicted where the dual N-factor indicator function, $\mathcal{I}(N_{TS}, N_{CF})$, reaches the unity value

$$\mathcal{I}(N_{TS}, N_{CF}) \equiv \left(\frac{N_{TS}}{N_{TS,c}}\right)^{a_{TS}} + \left(\frac{N_{CF}}{N_{CF,c}}\right)^{a_{CF}} = 1$$

- $N_{TS,c} = 6$ based on wing body experiments in the National Transonic Facility[8]
- $N_{CF,c} = 6$, $a_{TS} = a_{CF} = 3$ based on previous calculations for CRM-NLF with imposed transition fronts at measured locations[9]

---

[8] J. Crouch et al. *Assessment of the National Transition Facility for Natural Laminar Flow Testing*. AIAA Paper 2010-1302. 2010. DOI: 10.2514/6.2010-1302.

[9] P. Paredes et al. *Transition Analysis for the CRM-NLF Wind Tunnel Configuration*. AIAA 2021-1431. 2021.

[10] D. Arnal. "Boundary layer transition: Prediction based on linear theory". In: *Special course on Progress in Transition Modeling. AGARD. R-793.* 1994, pp. 1–62.

Iterative Method for Transition Modeling

- Viscous-inviscid interactions lead to movement of shock fronts and leading-order changes in C_p distribution between fully-turbulent (FT) and imposed transition (IT) solutions

Iterative method to model transitional flow over transonic configurations

1. Calculate FT mean flow and extract the shock front as the predicted transition front
2. Calculate mean flow with IT front set at predicted front and extract the new shock front
3. Perform stability analysis along streamlines up to the IT front and define a new transition front by taking the point on each streamline where
   - the dual N-factor reaches unity upstream of the IT front
   - the shock front is reached
4. Check convergence and go to step 2 if not satisfied

- Automatic extraction of the shock front at the stronger shock location
- Extrapolation of the dual N-factor values near IT front
- Predicted transition front updated with 0.75 underrelaxation and a 3-point smoothing

Outline

1 Motivation

2 Theory

3 Results

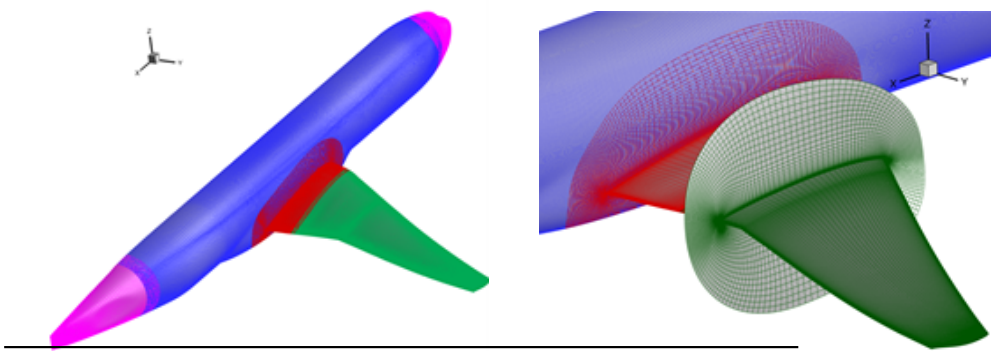
4 Summary and Concluding Remarks

Flow Conditions and Computational Details

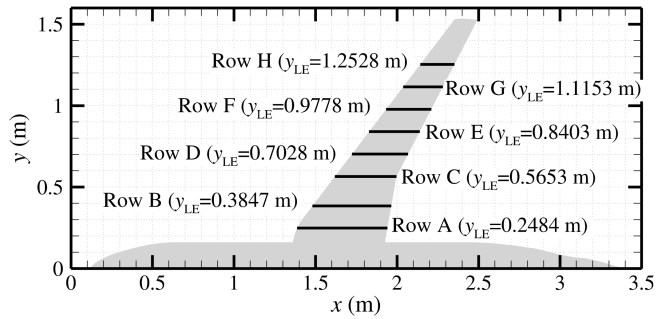
- The NASA OVERFLOW 2.3b solver[11]: NS solver for structured, overset grids
- Fully turbulent (FT) and imposed transition (IT) solutions with SA RANS model
- Flow conditions given by the AIAA Transition Modeling and Prediction workshop
- Adiabatic wall and constant $M_\infty = 0.8565$.

Case	AoA (°)	Re_{MAC} (10^6)	M_∞	$\bar{T}_\infty$ (K)	Re_∞ (10^6 m^{-1})
I	1.448	14.84	0.856	241.7	40.73
II	1.980	14.81	0.856	242.0	40.66
III	2.461	14.78	0.856	242.0	40.56
IV	2.937	14.72	0.856	243.0	40.41

- Surface and wing grid (120×10^6 total points)



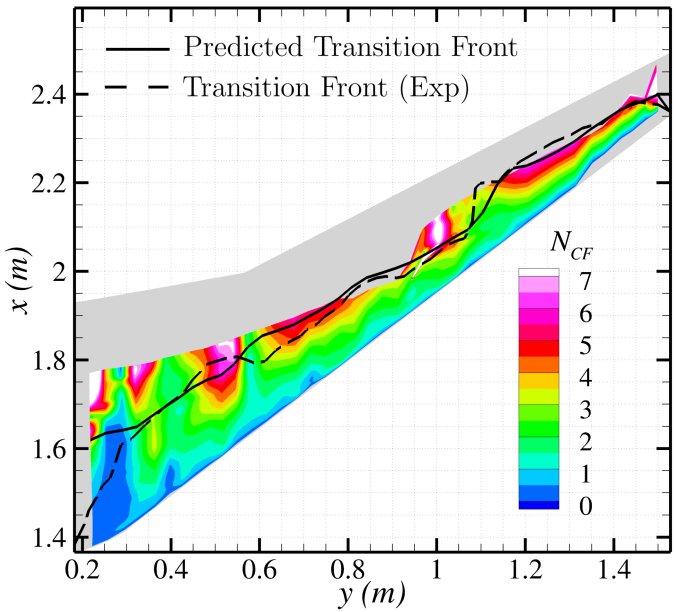
- Span locations of ports

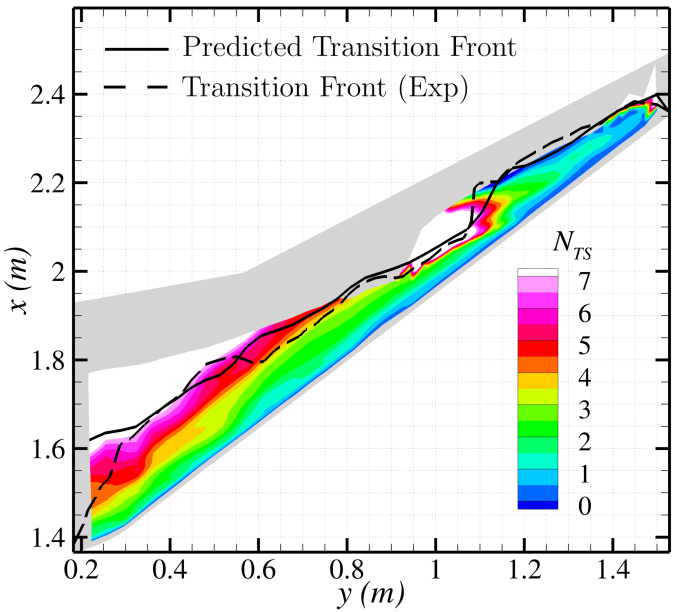


[11] H Nichols and PG Buning. *User's manual for OVERFLOW 2.3*. 2019. URL: https://overflow.larc.nasa.gov/home/users-manual-for-overflow-2-3/.

Linear amplification of CF and TS

- **Case I ($Re_{MAC} = 15$M, $AoA = 1.45°$), Iteration 1**
- N-factors computed with PSE along 40 streamlines
  - N_{CF} ($\omega = 0$)
  - N_{TS} ($\beta = 0$)

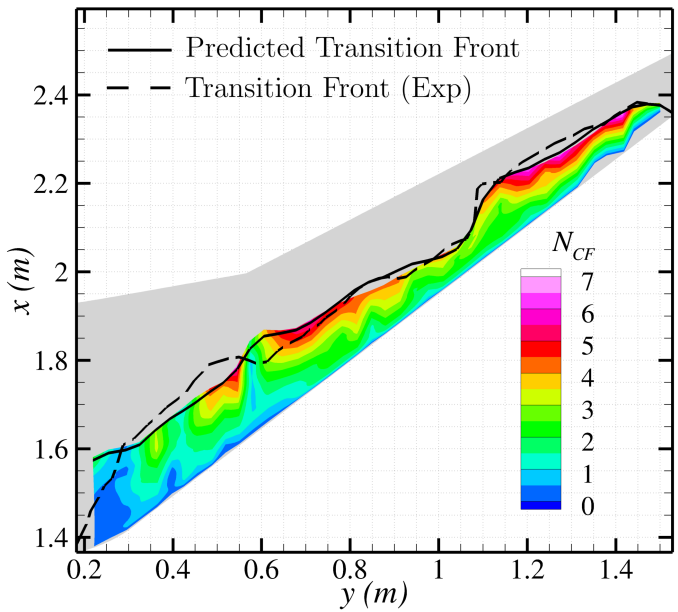


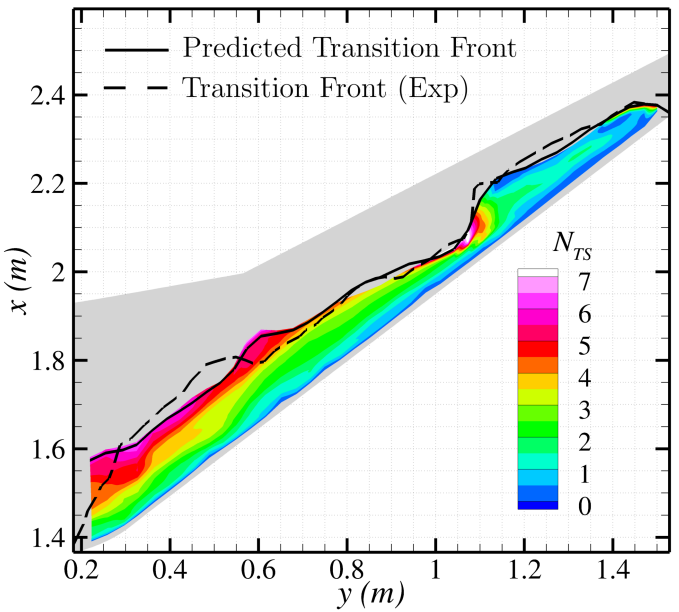


- Large values of N_{CF} in midspan and outboard regions but shock limited
- Region inboard of Yehudi break mainly dominated by TS with $N_{TS} \approx 7$
- Shock shift ($y \in (0.95, 1.1)$ m) corrected due to high N in separation region

Linear amplification of CF and TS

- **Case I ($Re_{MAC} = 15$M, $AoA = 1.45°$), Iteration 3**
- N-factors computed with PSE along 40 streamlines
  - N_{CF} ($\omega = 0$)
  - N_{TS} ($\beta = 0$)

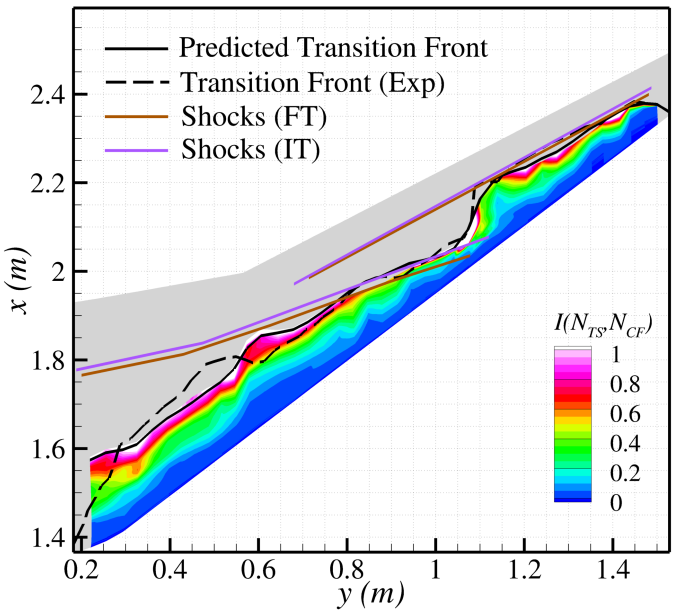


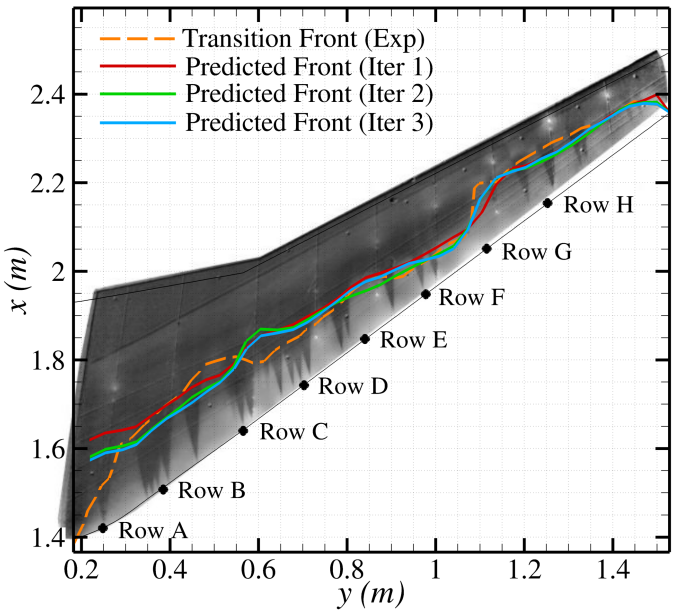


- N_{TS} and N_{CF} slightly change from iteration 1 to 3 over the laminar region
- N_{TS} peak near $y = 1.1$ m corresponds to small separation due to the smoothing of the predicted front

Transition and Shock Fronts

- **Case I ($Re_{MAC} = 15$M, $AoA = 1.45°$)**
- Experimental transition fronts manually extracted from TSP images[12]
- Shock fronts extracted at strong C_p gradient
  - Dual N-factor (Iteration 3)
  - Predicted transition fronts



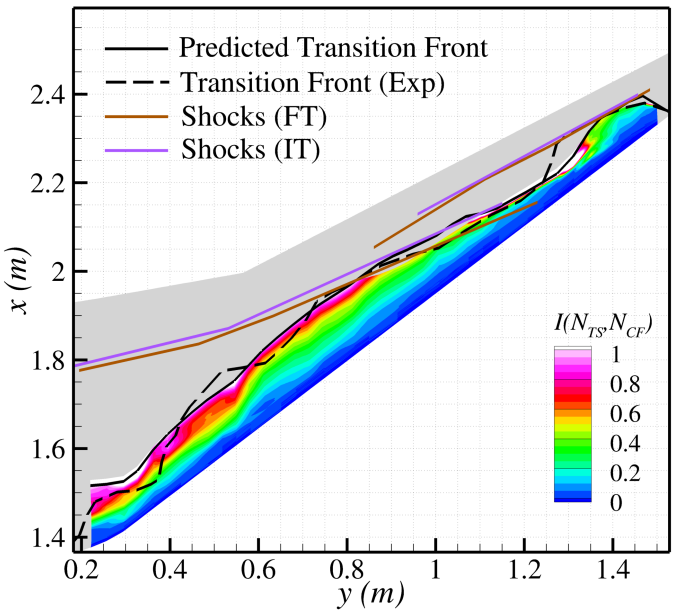


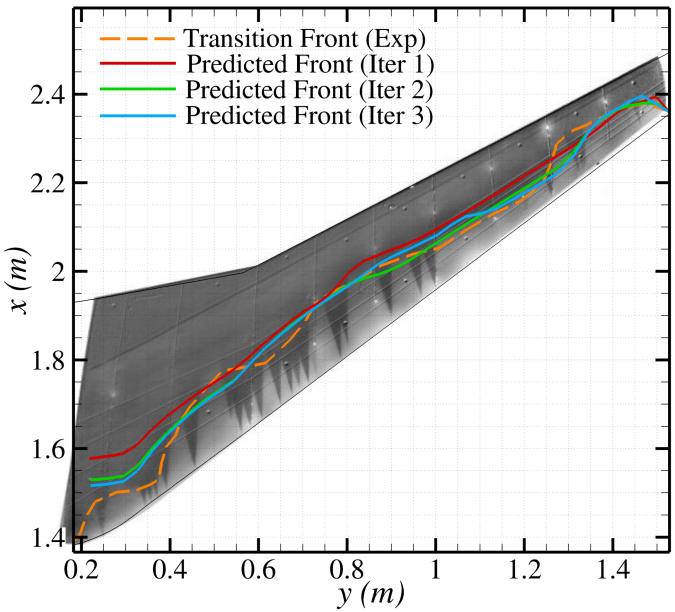
- Shock front locations significantly different between FT and IT solutions
- Shock-limited transition front in outboard region
- General acceptable agreement with experimental transition fronts across AoAs

[12] M. Lynde, R. Campbell, and S. Viken. *Additional findings from the common research model natural laminar flow wind tunnel test*. AIAA Paper 2019-3292. 2019. DOI: 10.2514/6.2019-3292.

Transition and Shock Fronts

- **Case II ($Re_{MAC} = 15$M, $AoA = 1.98°$)**
- Experimental transition fronts manually extracted from TSP images[12]
- Shock fronts extracted at strong C_p gradient
  - Dual N-factor (Iteration 3)
  - Predicted transition fronts



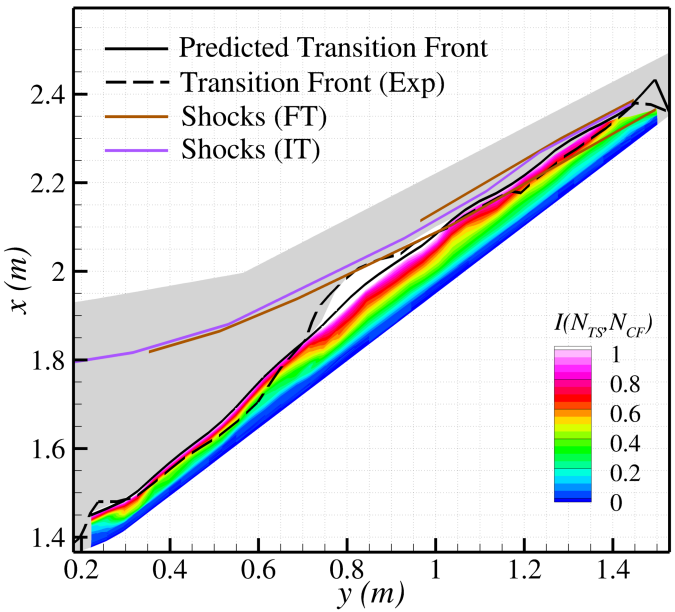


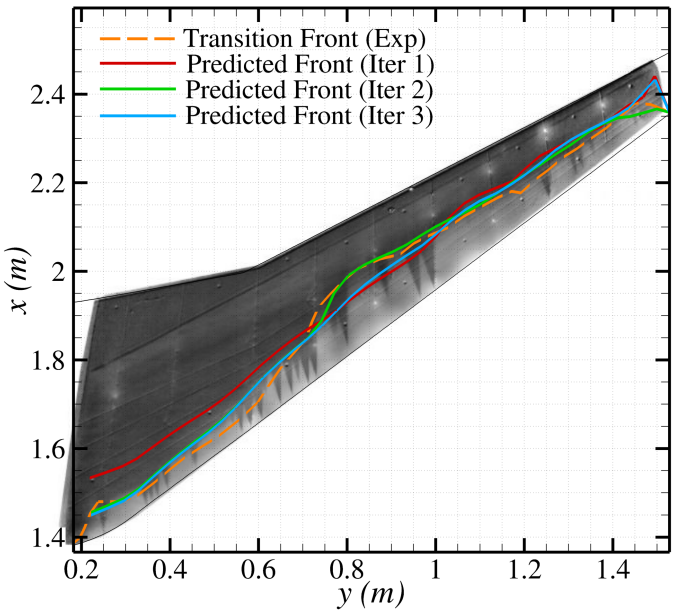
- Shock front locations significantly different between FT and IT solutions
- Shock-limited transition front in outboard region
- General acceptable agreement with experimental transition fronts across *AoA*s

[12] M. Lynde, R. Campbell, and S. Viken. *Additional findings from the common research model natural laminar flow wind tunnel test*. AIAA Paper 2019-3292. 2019. DOI: 10.2514/6.2019-3292.

Transition and Shock Fronts

- **Case III ($Re_{MAC} = 15$M, $AoA = 2.46°$)**
- Experimental transition fronts manually extracted from TSP images[12]
- Shock fronts extracted at strong C_p gradient
  - Dual N-factor (Iteration 3)
  - Predicted transition fronts



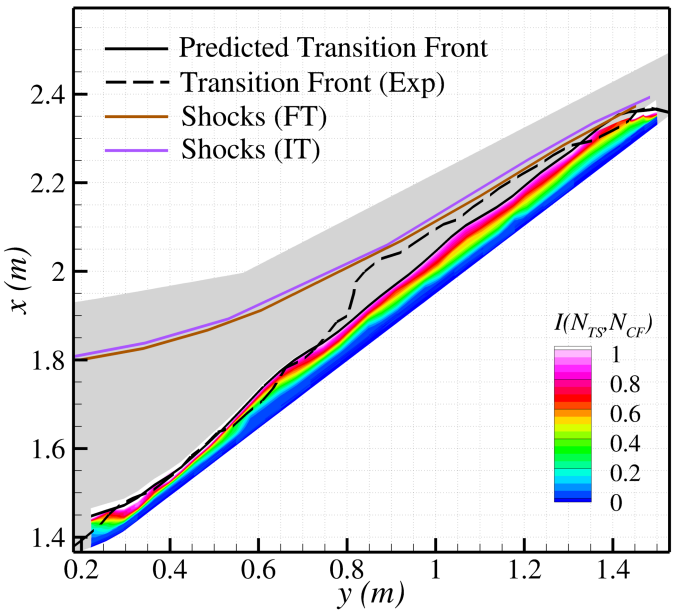


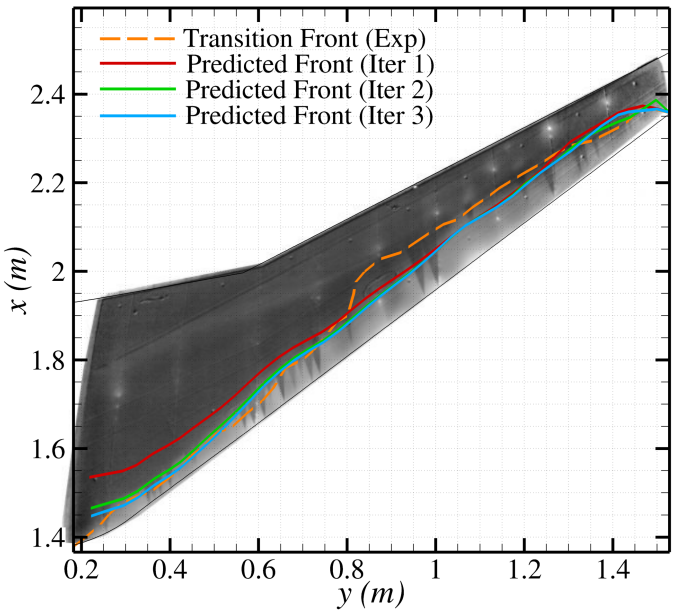
- Shock front locations significantly different between FT and IT solutions
- Shock-limited transition front in outboard region
- General acceptable agreement with experimental transition fronts across *AoA*s

[12] M. Lynde, R. Campbell, and S. Viken. *Additional findings from the common research model natural laminar flow wind tunnel test*. AIAA Paper 2019-3292. 2019. DOI: 10.2514/6.2019-3292.

Transition and Shock Fronts

- **Case IV ($Re_{MAC} = 15$M, $AoA = 2.94°$)**
- Experimental transition fronts manually extracted from TSP images[12]
- Shock fronts extracted at strong C_p gradient
  - Dual N-factor (Iteration 3)
  - Predicted transition fronts



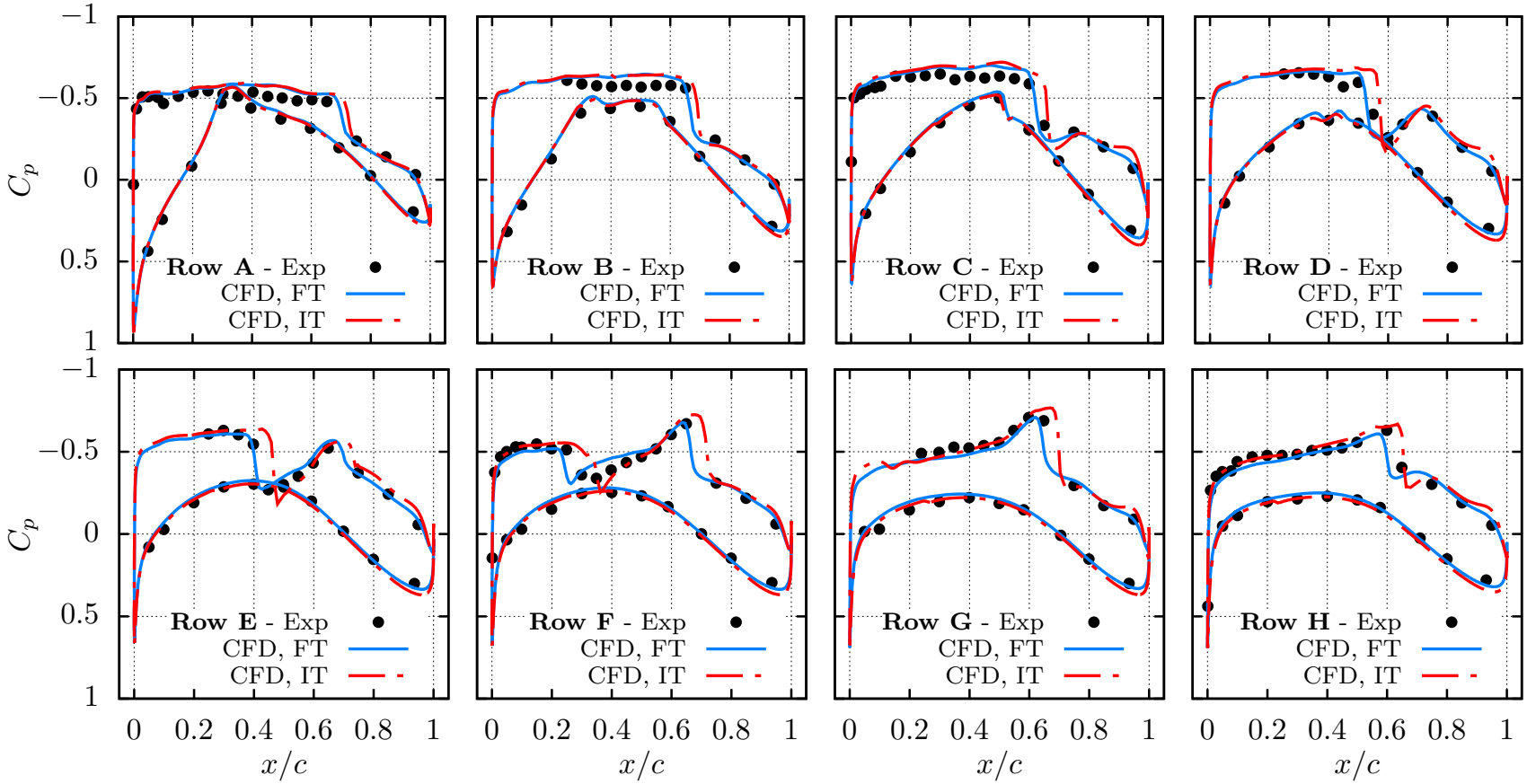


- Shock front locations significantly different between FT and IT solutions
- Shock-limited transition front in outboard region
- General acceptable agreement with experimental transition fronts across *AoA*s

[12] M. Lynde, R. Campbell, and S. Viken. *Additional findings from the common research model natural laminar flow wind tunnel test*. AIAA Paper 2019-3292. 2019. DOI: 10.2514/6.2019-3292.

Pressure Coefficient

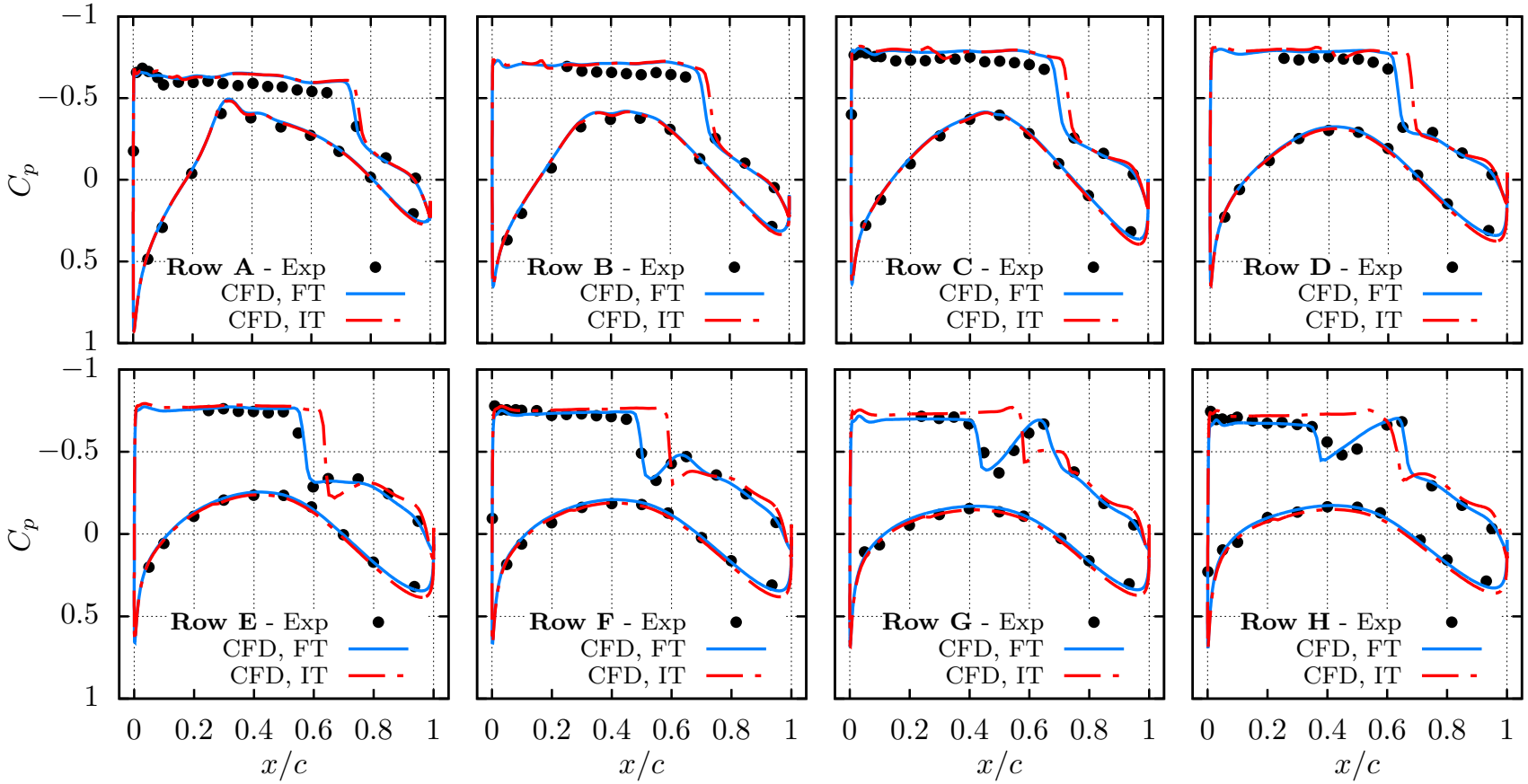
- C_p at selected span locations
- Case I ($Re_{MAC} = 15\text{M}$, $AoA = 1.45°$)



- Reasonable agreement between CFD solutions and experimental measurements
- Agreement within the laminar region is not visually altered
- IT solution shows delayed shock locations wrt FT and Exp

Pressure Coefficient

- C_p at selected span locations
- Case III ($Re_{MAC} = 15 \times 10^6$, $AoA = 2.46°$)



- Reasonable agreement between CFD solutions and experimental measurements
- Agreement within the laminar region is not visually altered
- Double shock system becomes a single shock for the IT case III solution

Outline

1 Motivation

2 Theory

3 Results

4 Summary and Concluding Remarks

Summary

- Transition modeling method based on iterative procedure
  - begins with imposed transition at the shock front extracted from fully turbulent solution
  - updates the transition front based on the dual N-factor method with nonorthogonal PSE that accounts for the linear amplification of planar TS and stationary CF waves
- Predicted transition fronts favorably agree with experimental data
- Three iterations lead to nearly converged solutions
- Pressure coefficients agree well with experimental data, although IT solutions show a consistent shift of shock location
  - pressure ports were likely tripping the boundary layer
- Future work:
  - Reynolds number effects
  - Surface curvature and nonparallel effects by comparing with equivalent results based on parallel LST analysis
  - Quantify uncertainty in the experimental transition fronts extracted from the TSP images

Thank you for your attention

- Acknowledgements
  - This research was sponsored by the NASA Transformational Tools and Technologies (TTT) Project of the Transformative Aeronautics Concepts Program (TACP) under the Aeronautics Research Mission Directorate (ARMD)
  - Resources supporting this work were provided by the NASA High-End Computing (HEC) Program through the NASA Advanced Supercomputing (NAS) Division at Ames Research Center and by the LaRC K Cluster at Langley Research Center.



